*30th EPS Conference on Contr. Fusion and Plasma Phys., St. Petersburg, 7-11 July 2003 ECA Vol. **27A**, P-1.10*

First results from the WEGA stellarator

J. Lingertat, K. Horvath, H. P. Laqua, M. Otte, Y. Podoba, F. Wagner

Max-Planck-Institut für Plasmaphysik, Euratom Association, Wendelsteinstr. 1, 17491 Greifswald, Germany

Introduction

The WEGA (Wendelstein Experiment in Greifswald für Ausbildung) is a classical l=2, m=5 stellarator (R=0.72m, a=0.19m). It has been operated in a modernised version since 2001 at IPP. The machine is mainly used for educational training, testing of new diagnostic equipment, for basic research in plasma physics and for testing and continuous operation of the new technical infrastructure of the institute.

The plasma in WEGA is ignited and heated from the low-field side by ECRH at 2.45 GHz (O-mode). The maximum power available is 6 kW. Typically, the resonant field of B_o = 87.5mT (1st harmonic) or of $B_0/2$ (2nd harmonic) is located at the centre of the vacuum vessel. ι_0 is varied between 0.2 and 0.5. The standard length of a discharge is a few minutes. Working gases are H_2, He and Ar.

The established operational limits for the magnetic fields in steady state operation are $I_{tor} \leq 2.6$ kA ($B_{tor} \leq 0.37$ T) and $I_{hel} \leq 3.5$ kA ($\iota_0 \leq 0.18$ at $I_{tor} = 2.6$ kA).

The following diagnostics are operational: residual gas analyser, Langmuir probe with slow and fast manipulator, H_α - detector, interferometer and optical overview spectrometer.

Plasma profiles

One of the basic diagnostics implemented at WEGA is a Langmuir probe. Given the low power density of the plasma the probe can be used throughout the whole cross-section to measure n_e, T_e and Φ_{plasma} as a function of radius. Different probe geometries and arrangements have been used to study specific features of probe physics and to develop procedures for the evaluation of the probe characteristics.

One common feature of all characteristics is the absence of ion current saturation. A model capable to fit the measured characteristics relies on the assumption of a two-temperature Maxwellian distribution of electron energies [1]. This assumption is consistent with the used heating method. Typically, ECR heated discharges show a high electron energy tail. Fig. 1 shows a measured Langmuir characteristic together with the fitting curve. Parameters obtained by the fitting procedure are T_e and n_e for the slow (s) and fast (f) component, the ion saturation current, the floating and plasma potential.

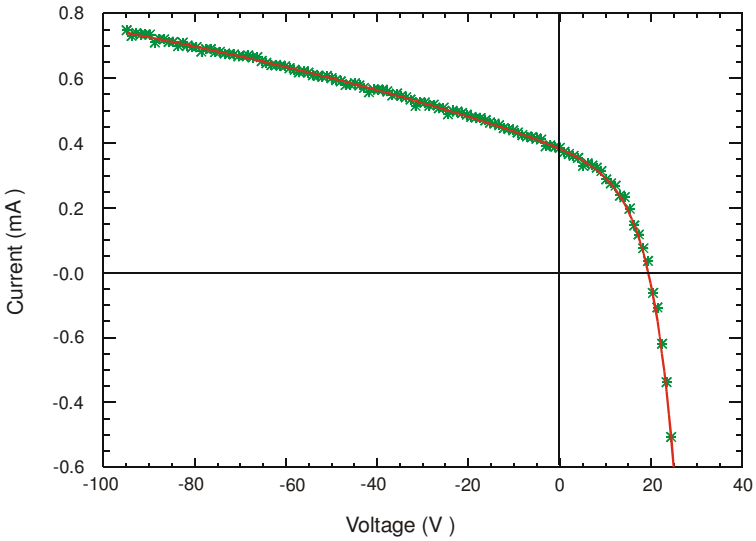

Fig. 1
Langmuir probe characteristic (green) and two-temperature fit (red),
$T_{e,s}$ = 4.7 eV, $T_{e,f}$ = 143 eV,
$n_{e,s} = 1.84\times10^{17}$ m^{-3},
$n_{e,f}/n_{e,s}$ = 0.25%,
I_{sat} = 1.1 mA,
Φ_f = 19.9 V, Φ_p = 46.0 V

Fig. 2 shows as an example radial profiles obtained by Langmuir probe measurements. The maximum n_e achieved in discharges with full heating power is above 10^{18} m^{-3} and is much higher than the cut-off density ($n_{e,cut\text{-}off} = 7.5\times10^{16}$ m^{-3}). Typical electron temperatures of the slow component are in the range of 5 eV - 10 eV, whereas the fast T_e – component reaches values of a few 100 eV. The floating potential shows a negative dip near the LCFS which is observed in many plasma experiments and may be caused by a high concentration of fast electrons in the low density edge. Usually, the fitting results for $T_{e,f}$ and $n_{e,f}$ have rather large error bars, probably caused by the low concentration of fast electrons ($n_{e,f}/n_{e,s} \ll 1$).
Using the data from Fig. 2 and assuming T_i = 0.3 eV [2] the following estimates can be made: $\rho_e = 1.2\times10^{-4}$ m, $\rho_i = 8.1\times10^{-3}$ m, $\lambda_{ei} = 0.28$ m, $\lambda_{ii} = 1.4\times10^{-3}$ m, $\tau_E \geq 0.05$ ms, τ_{ISS95} = 0.15 ms, $\beta = 0.17\%$, degree of ionisation $\alpha \geq 85\%$.

Plasma heating

The microwave is transmitted from the magnetron to the torus via a rectangular waveguide. Near the machine the rectangular waveguide changes to a circular one, which finally enters the torus radially at mid-plane as a stainless steel tube with an inner diameter of 85 mm. The calculated emission pattern of such an antenna shows that most power is emitted in axial direction, which means perpendicular to the magnetic flux surfaces. The emission pattern can be changed by cutting the end of the antenna tube under an angle of 45°. The maximum power is then emitted under an angle of ~ 10°.

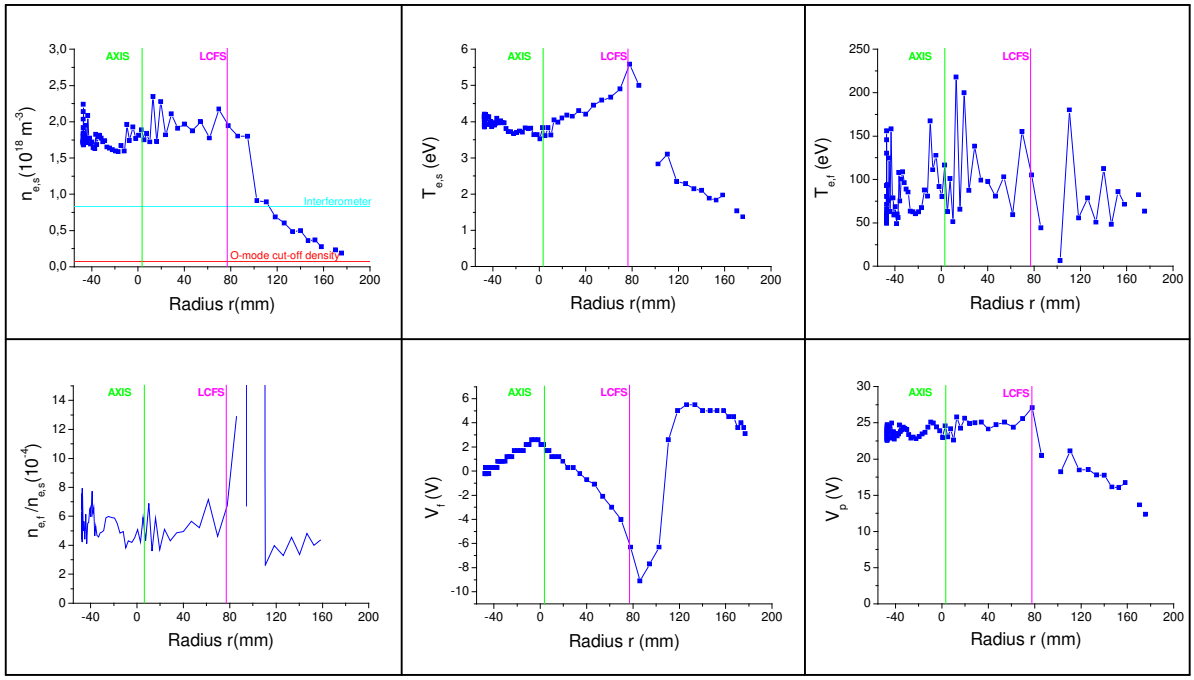

Fig.2 Radial profiles in Ar (P = 6 kW, B = 61.2 mT, ι_0 = 0.2, $p_n = 1.4\times10^{-3}$ Pa, I(B_z) = 12 A)

Using the two types of antennas the following heating scenarios have been investigated:

- The 1st harmonic X–mode together with the 90°-antenna causes a standing wave to develop between the low density cut-off layer and the antenna, resulting in extremely hollow plasma profiles, highly unstable discharges and overheating of the antenna port. The plasma is heated mainly outside the LCFS. The maximum densities achieved under this heating scheme are $n_{e,\,max} \leq n_{x,\,cut\text{-}off}$.
- The 1st harmonic O-mode together with the 90°-antenna gives still hollow profiles of T_e and n_e where the maxima are located outside the separatrix. Thereby the maximum density is always above the cut-off density for O-mode ($n_{e,max} \leq 1.5\times n_{o,cut\text{-}off}$). The hollowness of profiles may be explained by assuming repeated reflections of the wave between the cut-off layer outside the LCFS and the inner wall. The wave energy is absorbed at the upper-hybrid layer, which is located outside the LCFS.

  A small part of the wave power is emitted under an angle of α_{opt}=45° which is the optimum angle for conversion into X-mode at the cut-off layer followed by a second mode conversion at the upper-hybrid resonance into a Bernstein wave (OXB process). The Bernstein wave freely propagates into the plasma centre, where it is absorbed.

- For the 2nd harmonic O-mode α_{opt} is smaller (α_{opt}=35°). More power can undergo the OXB process and heat the plasma centre. Indeed, the n_e profile becomes less hollow or even peaked ($n_{e,max} \geq 5 \times n_{o,cut\text{-}off}$). The T_e profile stays hollow, although the temperature maximum moves with increasing heating power inside the LCFS.
- Using the 45° antenna even more power is emitted in the favourable direction. With this antenna the highest densities and temperatures have been obtained so far (example in Fig.2).

The efficiency of OX-conversion for the three cases discussed above has been estimated by calculating the emission pattern of the antenna with the HFSS code and folding the result with the OX-transmission function T from [3]. We find for the three O-mode cases described above conversion efficiencies of 6%, 14% and 11%. However, since the wavelength at 2.45 GHz (λ~12 cm) is comparable with the minor radius and most models of the OXB-process assume $\lambda << a$ or even $\lambda << n_e/\nabla n_e$, the obtained values for the conversion efficiency are rough estimates only.

Future plans

At present, several new types of antennas are under design. The aim is to increase the fraction of power which is converted into Bernstein mode and absorbed in the plasma centre. The OXB process will be further investigated by measuring the wave field inside the plasma and the ECE emission. An additional heating method, Helicon wave heating, is under preparation.

The assumption of a high energy electrons will be verified by soft X-ray measurements. A study of transport and fluctuations in magnetic islands have just been started [4]. Furthermore, additional diagnostics are in the commissioning or designing phase: bolometer camera, high resolution optical spectrometer for T_i and flow velocity measurements, laser absorption spectroscopy for measurement of the temperature of neutrals.

References

[1] Stangeby, P.C., Plasma Phys.Control. Fusion 37 (1995) 1031.
[2] Gandy, R.F. et al., Physics of Plasmas 5 (1998) 2405.
[3] Mjølhus, E., J. Plasma Phys. 31 (1984) 7.
[4] Otte, M. et al., 30th EPS Conference Plasma Phys. Control. Fusion (2003) P-1.9.

Acknowledgement

The technical support of D. Aßmus and N. Paschkowski is gratefully acknowledged.